JAAS

View Online / Journal Homepage
Dynamic Article Links

Cite this: DOI: 10.1039/c2ja30021d

www.rsc.org/jaas

PAPER

Silver nanoparticle characterization using single particle ICP-MS (SP-ICP-MS) and asymmetrical flow field flow fractionation ICP-MS (AF4-ICP-MS)†

Denise M. Mitrano,*[a] Angela Barber,[a] Anthony Bednar,[b] Paul Westerhoff,[c] Christopher P. Higgins[d] and James F. Ranville[a]

Received 27th January 2012, Accepted 12th April 2012
DOI: 10.1039/c2ja30021d

Methods to detect, quantify, and characterize engineered nanoparticles (ENPs) in environmental matrices are highlighted as one of the areas of highest priority research needs with respect to understanding the potential environmental risks associated with nanomaterials. More specifically, techniques are needed to determine the size and concentration of ENPs in a variety of complex matrices. Furthermore, data should be collected at environmentally and toxicologically relevant concentrations. Both single particle inductively coupled plasma mass spectrometry (SP-ICP-MS) and asymmetrical flow field flow fractionation (AF4) ICP-MS offer substantial advantages for detecting ENPs and assessing many of the above parameters in complex matrices over traditional characterization methods such as microscopy, light scattering, and filtration. In this study, we compared the ability of two emerging techniques to detect well characterized, monodisperse silver ENPs and examined their overall applicability to environmental studies specifically with respect to their: (A) size and concentration detection limits, (B) resolution and (C) multi-form elemental analysis. We find that in terms of concentration detection limit (both, on a mass basis and particle number basis) SP-ICP-MS was considerably more sensitive than AF4-ICP-MS (ng L^{-1} *vs.* μg L^{-1}, respectively), and offers the unique ability to differentiate dissolved and nanoparticulate fractions of total metal. With a variety of optimization parameters possible, AF4-ICP-MS can detect a much smaller NP size (2 nm *vs.* 20 nm for SP-ICP-MS), provides the possibility for greater size resolution.

Introduction

Nanomaterials have great potential in both industrial and commercial sectors, becoming useful products for society either when used alone or when integrated into larger products (*e.g.* consumer goods, foods, pesticides, pharmaceuticals, and personal care products, among others). The ubiquitous use of goods containing nanomaterials may compromise the health of many ecosystems. A number of life cycle assessments concluded that a significant amount of nanomaterials may enter aquatic systems in both the United States and Europe.[1–3] Metal-containing nanoparticles (NPs) form a particularly prominent group, specifically Ag NPs, as they are the fastest growing category of engineered NPs (ENPs). Furthermore, ionic silver (Ag^+) release from Ag NP bearing plastics and textiles may also be substantial enough to cause considerable concern.[4] However, the potential biological impacts of Ag NPs are not solely due to their release of Ag^+ alone, as NP size,[5,6] chemical composition, surface structure,[7] solubility, shape,[8] and aggregation[9] have been documented as important factors controlling their biokinetics. Confounding the issue, the release of Ag^+ from Ag NPs is likely dependent on the given environmental parameters: concentration of ligands, interactions with organic matter, ionic strength, and pH.[10]

Our lack of understanding of potential environmental impacts of nanomaterials is, in part, due to the difficulties of nanoscale detection that exist in environmental and biological samples. The systems are complex and involve heterogeneous matrices, all of which may contain very low levels of ENPs. There are nearly universal calls within the nanotechnology community for improvements in regards to nanometrology, and the need to fill in many existing knowledge gaps in detection, characterization, and quantification of nanomaterials. Although there have been recent strides in the analysis of ENPs in complex matrices,[11] the

[a]*Colorado School of Mines, Department of Chemistry and Geochemistry, Golden, CO, USA. E-mail: jranville@mines.edu*
[b]*U.S. Army Engineer Research and Development Center, Vicksburg, MS, USA*
[c]*Arizona State University, School of Sustainable Engineering and the Built Environment, Tempe, AZ, USA*
[d]*Colorado School of Mines, Department of Civil and Environmental Engineering, Golden, CO, USA*
† Electronic supplementary information (ESI) available. See DOI: 10.1039/c2ja30021d

most common detection and characterization methods used for assessing particle concentration and size distributions, namely microscopy,[12] chromatography,[13] centrifugation,[14] laser light scattering,[15] and filtration[16,17] are inadequate for the study of NPs in complex systems.[18] One particular analytical challenge is distinguishing NPs from other constituents of the matrix such as natural particles, humic substances, and debris.[19] Another problem is that method detection limits are higher for many techniques than expected exposure concentrations.[20] Differentiating dissolved and nanoparticulate forms of the metal, as well as possible NP coatings and aggregates, are also key aspects that should be investigated. Here, we compare and contrast two methods that address a number of challenges for nanometrology: single particle inductively coupled plasma mass spectrometry (SP-ICP-MS) and asymmetrical flow field flow fractionation ICP-MS (AF4-ICP-MS). Of note, NP shape is also thought to influence toxicity, but this is a parameter that these methods do not currently address.

The operation of the ICP-MS instrument in the single particle mode provides a means of detecting individual NPs. The technique is outlined in brief here, as several recent publications delve into the specific methods and theory more completely.[21–23] SP-ICP-MS relies on the extremely sensitive elemental detection capability of ICP-MS, but in contrast to traditional ICP analysis techniques, thousands of individual intensity readings are acquired, each with a very short dwell time (~10 ms). When analyzing an unacidified, NP-containing solution, instead of measuring elemental concentration representative of the bulk sample, the intensity readings can be collected as a function of time, where pulses above the background represent the measurement of an individual NP. The SP-ICP-MS technique may enable simultaneous determination both of dissolved metal concentrations as well as NP concentration and size (to as low as 20 nm), all at very low (ng L^{-1}) concentrations. The technique requires little sample preparation and little additional method development for a given matrix and/or analyte. However, the technique is highly dependent on the signal to noise ratio of a given ICP-MS, which may significantly hinder analysis of smaller sized Ag NPs.

Field flow fractionation consists of a suite of high resolution elution techniques which, depending on the type of field applied and mode of operation, allows separation and sizing of macromolecules, submicron colloids, and particles of 2–100 mm.[24] The separation process is similar to chromatography except that the separation is based on physical forces as opposed to chemical interaction. All separation is performed in a thin channel with laminar flow under the influence of a perpendicular field. AF4 was chosen for this study because it is the most widely used subset of FFF techniques for environmental analysis and is highly versatile for a range of both natural and manufactured NPs. As outlined in Baalousha and Lead,[25] the increased use of flow-FFF can be related to: (i) the wide size range that can be fractionated either of natural colloids (1–1000 nm) or natural and manufactured NP (1–100 nm);[26] (ii) the ability to change carrier solutions with respect to pH and ionic strength as to match the carrier solution with sample composition;[27,28] and (iii) the possibility of both on-line hyphenation to a wide range of detectors as well as collection of sample fractions for further off-line analysis.[25,29,30] Several reviews have been released touting the broad range of environmental,[31] bio,[32,33] and nanoparticle[20,34–36] applications for FFF-ICP-MS. Furthermore, the capability of multi-element analysis is an added benefit when coupling FFF with mass spectrometry. Though literature is scarce for engineered nano-specific studies, there is a growing use of FFF for nanoecotoxicology, with increasing interest concerning characterization methodology for environmental and biological risk evaluation. Notably, recent studies to characterize quantum dots[37] and NPs[38–40] in biological media before and after exposure, as well as environmental samples,[35,41,42] have shown promising results when using FFF-ICP-MS.

The goal of this present study is to compare the advantages and limitations of the two techniques. To make the comparison simple and objective, a list of criteria were made on which to determine each techniques' capabilities. These criteria include: (A) size and concentration detection limit, (B) size resolution and (C) multi-form metal analysis (such as distinguishing NP *vs.* dissolved constituents, NP complexes and aggregates, and multi-metals analysis). By using well characterized, monodisperse Ag NPs, we used systematic dilution, mixture analysis (both multi-size NP and Ag^+/Ag NP mixtures), and spiked complex matrices, to assess the smallest particle size and concentration determined by each technique, the ability of the techniques to differentiate between sample constituents, and their abilities to track NP transformations.

Materials and methods

Materials

Silver nanoparticles (NanoXact) were acquired in sizes of 20, 40, 60, 80 and 100 nm diameters (Nanocomposix, San Diego, CA). Suspensions were supplied at a nominal concentration of 20 mg Ag L^{-1} and were stabilized in aqueous 2 mM citrate per the manufacturer. Accompanying size information (Dynamic Light Scattering and Transmission Electron Microscopy) verified these particles to be monodisperse with the nominal sizes being: 20 ± 1.9 nm, 40 ± 3.6 nm, 60 ± 5.3 nm, 80 ± 6.8 nm, and 100 ± 9.4 nm though further characterization using a disc centrifuge showed the size of the 100 nm particles to be 91.3 ± 0.6 nm with an associated secondary particle with an equivalent diameter of 109.7 ± 0.8 nm.[43] Ag NP suspensions were made by diluting the stock solutions with 18.3 M ohm Nanopure water to final concentrations ranging from 2 to 500 ng Ag L^{-1}. Dissolved Ag standards (High-Purity Standards; QC-7-M), used for calibration, were diluted in 1% nitric acid (Optima grade) to concentrations ranging from 0.1 to 1 μg L^{-1}. This standard was also used as the dissolved Ag fraction when studying Ag^+/Ag NP mixtures. Bovine serum albumen (BSA; Sigma-Aldrich) was used for particle stabilization in studies of dissolved Ag complexation using AF4-ICP-MS.

Methods

Instrumentation – SP-ICP-MS. A Perkin Elmer NexION 300Q was used for single particle (SP) analysis. Operating conditions were optimized to produce maximum Ag intensity by modifying the sample introduction rate and changing the nebulizer gas flow. ^{107}Ag was continuously monitored for detection, with integration dwell times ranging from 0.1 to 20 ms per reading. The length of

dwell time was found to contribute significantly to the quality of data, where 10 ms was optimal. Intensity data were recorded using the ICP-MS software and were exported to Excel (Microsoft) for data handling and processing.

Instrument calibration was achieved by analysis of a blank and four dissolved Ag solutions ranging from 0 to 1 μg L^{-1} with data collected in the SP mode. The ^{107}Ag intensity of Ag for each solution was then averaged from the entire length of the standards analysis (typical times). No internal standard was employed, as only ^{107}Ag was quantified during the run. To ensure the absence of significant instrumental drift over time, a single 100 ng L^{-1} Ag dissolved calibration check standard was run in SP mode for every ten Ag NP samples analyzed.

Instrumentation – AF4-ICP-MS. For AF4-ICP-MS analysis, both a Perkin Elmer Elan 6100 and a Perkin Elmer NexIONQ were used. Standard operating and tuning procedures were used in maintaining and calibrating the instrument. Only one Ag isotope was monitored for detection (^{107}Ag), with an integration time of 2000 ms, alternating with a Bi internal standard (with a dwell time of 1000 ms), resulting in data being collected at approximately one reading every 3 s for the entire length of the fractogram, which depending on experimental conditions, ranged from 40 to 80 minutes. An asymmetrical FFF, AF 2000 AT, from Post Nova Analytics (Salt Lake City, UT) was used with a 10 kDa regenerated cellulose membrane, changed approximately every 25 runs, and with a carrier fluid consisting of 0.025% FL-70 surfactant and 0.01% sodium azide as an antibacterial agent. A 100 μL injection loop was used to load samples onto the channel, and flushed continuously throughout analysis. The AF4 was directly plumbed into the ICP-MS. The channel flow conditions allowed direct connection of the AF4 effluent to the ICP-MS nebulizer without a flow splitter. The AF4 separation conditions varied through method development, but were predominately a 10 min relaxation period (focusing step), followed by 40–80 min elution (0.7–1.0 mL min^{-1} cross flow and 1.0 mL min^{-1} detector flow), and a 10 min flush (field-off, 1.0 mL min^{-1}) between each experimental run.

Data collection, conversion to particle size, and quality of analysis

SP-ICP-MS. The theoretical basis of single particle detection has been outlined by Degueldre *et al.*[44–46] with further refinement and development in several recently published articles[21–23] that discuss specific aspects and applications of the technique. The fundamental assumption behind SP-ICP-MS is that at a sufficiently short dwell time and low particle number concentration, a pulse will represent a single particle event. The number of pulses can be directly correlated to the number concentration of particles (particle number per volume) and the intensity of the pulse (*i.e.* height) can be related to the particle size through particle mass, by making assumptions about particle geometry. Converting pulse height to particle diameter hinges on the calculation of an efficiency factor (η, nebulization/transport efficiency) for the ICP-MS. This can be measured using a standard, well-characterized metal NP such as Au NP, where η is the percentage of detected particles in SP-ICP-MS mode *versus* theoretical (calculated) particle number as determined by the elemental concentration, size, and density. Sizing the unknown particles then takes several steps (Fig. S1†), where we relate NP pulse height to NP mass, and subsequently size. First, a calibration curve is made by plotting concentration *versus* instrument response of the dissolved analyte metal. Mass flux is then calculated by relating the dissolved calibration curve to the analyte mass that actually enters the plasma during each reading. Here, we relate signal intensity to a total mass transported into the plasma in a given dwell time through the transport efficiency (η) which is instrument-specific. Finally, pulse occurrences are determined for the NP sample, and individual pulses from this dataset can be transformed using the mass flux calibration curve to particle mass, which can then be converted to particle diameter, when assuming a spherical geometry. In this way, a consistent method to size any particle is used even if no monodisperse standards for the given particle exist.

For all SP-ICP-MS analysis, raw intensity data were plotted as intensity of pulse *versus* number of events to create a pulse distribution histogram. Very low intensity readings were considered to be instrument background, or, for slightly higher intensity values, dissolved metal. After background/dissolved metal was subtracted from the pulse intensity, NPs were sized using the process previously outlined. Pulses that register at higher intensities are associated with larger diameter NPs, which plot with approximate Poisson distribution around a mean as a function of NP size. Deviation from this shape may be an indication of particle coincidence in a given dwell time, or a polydisperse sample set, and thus would require further sample dilution and characterization to differentiate between these two occurrences, as will be discussed. Dwell time was optimized by analyzing both 40 nm and 100 nm Ag NP sample (100 ng Ag L^{-1}) at 0.1, 1, 5, 10, 15, and 20 ms dwell times. Similarity to expected peak shape, separation from the background, no evidence of incomplete particle analysis, and blank counts registering at a low intensity value were considered in choosing the best dwell time. Finally, the effect of tuning of the ICP-MS to optimize for a given metal, in this case Ag, on the performance of the SP-ICP-MS technique was investigated by adjusting ICP-MS parameters for maximum analyte sensitivity. We then analyzed 100 nm Ag NP (100 ng Ag L^{-1}) and compared the SP-ICP-MS data with standard tuning to optimized tuning approaches for Ag NP pulse intensities.

AF4-ICP-MS. Size fractionation in AF4 takes place in a thin channel, which is constructed using a polyester spacer (0.25–0.5 μm) enclosed between two plexiglass blocks, with one porous block (frit) on the lower side. The laminar channel (tip) flow, which carries the sample through the system, creates a parabolic flow velocity profile. A perpendicularly applied fluid cross flow pushes particles against the lower (accumulation) wall, which consists of a semi-permeable membrane on top of the lower ceramic frit. After the sample is injected, a focusing step occurs and the sample is concentrated near the entrance of the channel. After a set focusing time, the separation of the particles occurs during the elution phase of analysis. During the elution, the cross flow pushes particles against the membrane, while diffusion causes particles to move away from the wall and into higher velocity flow. The interplay between these two forces causes smaller particles to interact with the faster part of the parabolic

flow, resulting in size dependent elution from the channel. In this way, retention time can be directly related to particle size where shorter retention times coincide with smaller particle diameters. In theory, the balance of these forces can only be changed by varying the flow conditions or spacer thickness. Due to interactions between the analytes and the membrane, this balance can also be affected by the membrane composition and/or the carrier solution composition (surfactant, pH, or ionic strength). Manipulation of all physical and chemical variables can optimize fractionation with respect to resolution and sample recovery. However, presuming all particles in the sample are of regular (spherical) shape and have equal interaction with the membrane, the interpretation of the elution profile (fractogram) is straightforward. FFF theory or a simple linear calibration from retention time *versus* particles of known size (excluding the void peak), can be used to size all analyte particles that have similar behavior within the FFF channel.

The AF4-ICP-MS fractograms were evaluated for sample recovery, reproducibility, absence or minimal height of the void peak, and distance between void and analyte peaks (retention ratio), and separation between analyte peaks (resolution). We determined suitable parameters for the effective fractionation over the size range of Ag NP of interest in this study, but did not necessarily find the best possible run conditions, as the complete optimization of all parameters was not the objective.

Size, detection limit, and resolution experimental parameters

For SP-ICP-MS analysis of size, detection limit, and resolution, 40, 60, 80 and 100 nm Ag NPs were analyzed either individually, or in mixtures, at concentrations ranging from 2 to 500 ng L^{-1} (as Ag). Size detection limit was defined by separation of the NP histogram from the instrumental/dissolved metal background where the smallest detectable NP creates a pulse intensity greater than the mean background intensity plus at least three times its standard deviation. A concentration detection limit was defined as the lowest possible mass-based concentration that still produced a clearly defined histogram for a given NP size. Resolution in SP-ICP-MS was determined by finding the difference in the histogram means between the particles of interest, in counts, and dividing by the average width of the peaks in corresponding units, as seen in the equation below, where ΔI_r is the separation between peaks (in units of counts), and w_{av} is the average width of the two peaks. The resolution itself is instrument dependent, as instrument sensitivity dictates the pulse intensity for a given NP size, and so with an increase in instrument sensitivity, there will be a larger intensity difference between particle sizes.

$$R = \frac{\Delta I_r}{w_{av}}$$

A mixture of 20 and 40 nm Ag NPs, each at 100 μg L^{-1} (as Ag), was analyzed by AF4-ICP-MS, at the beginning and end of each day to ensure that membrane conditions did not change during the course of the day. This would be noted by a shift in elution time or a change in peak area (percent recovery). Subsequent studies on detection limit and resolution were performed using mixtures of 20 to 80 nm Ag NPs in concentrations ranging from 2.5 to 100 μg L^{-1}. A size detection limit for this technique was obtained by referring to literature, where particles as small as 2 nm have been sized.[25] A mass based detection limit was defined as the lowest possible concentration that still produced a fractogram where both particles sizes were distinguishable from the background using a typical injection volume (20–100 μL). Resolution was determined by determining the difference in peak maxima, in retention time (seconds), and dividing by the average width of the two peaks, in similar fashion to the resolution equation above. The results presented here can be considered typical of AF4-ICP-MS, but as noted, resolution can be easily altered by changing flow conditions and physical parameters, such as spacer thickness.

Multi-form analysis

Determining the effectiveness of differentiating between dissolved and nanoparticulate elements in a sample by SP-ICP-MS was accomplished by varying the concentrations of 0, 50, and 100 ng L^{-1} of combinations of Ag^+ and 100 nm Ag NPs. Once the determination between dissolved and NP fractions had been made, each fraction was quantified using the appropriate procedure. For the dissolved fraction, this was performed *via* a direct comparison to the dissolved calibration curve. However, for the NP fraction, once the mean dissolved background intensity was subtracted from the pulse intensity, the intensity was converted to mass by accounting for the transport efficiency, which subsequently enabled calculations of NP diameter and mass/number concentrations.

To test the capability of detecting NP surface modifications, NP aggregation, and dissolved complexes, we performed an experiment using AF4-ICP-MS, on protein-containing solutions. Bovine serum albumen (BSA), a protein that has numerous biochemical applications, was chosen as a surface modifier for Ag NPs because it is also reported to help disperse and stabilize NPs in complex media.[47] A solution containing 1.5 mg mL^{-1} BSA was added directly to an Ag NP mixture of 20 and 40 nm particles, at 100 μg L^{-1} each, and was allowed to equilibrate for 5 minutes before dilution (1000-fold) with DI water. The samples were sonicated for 5 min before analysis by AF4-ICP-MS, at 60 min intervals. The NP size was then compared to the daily standard (unaltered) NP mixture to determine if the BSA had adhered to the NP surface. Furthermore, association of Ag^+ to BSA was tracked by the increase in small particle size over time. A comparison of Ag NP aggregation was made between unaltered and BSA coated particles.

Results and discussion

Optimization for SP-ICP-MS

Instrument tuning has a clear impact on the sensitivity of SP-ICP-MS. After tuning optimization, the pulse intensity is significantly higher for the same 100 nm Ag NP solution (Fig. S2†). Optimization consisted of tuning the instrument for maximum sensitivity of ^{107}Ag by adjusting sample introduction flow rate and increasing nebulizer gas flow rate. The outcome gave operational conditions that were not necessarily optimal, as per standard daily ICP-MS tuning, such as higher than normal oxide levels, but these conditions yielded a significant increase in sensitivity during SP-ICP-MS analysis, with no apparent

analytical pitfalls. Additionally, through dwell time optimization analysis (Fig. S3†), we found that 10 ms dwell times consistently provided the most accurate results for a variety of sample concentrations and NP sizes.

Method optimization for AF4-ICP-MS

AF4 generally provides high-resolution separation for NPs, but there are a number of factors that may compromise separation, including particle aggregation within the channel and particle membrane interactions, among others. These factors must be taken into account during method optimization by choices of: (1) the carrier solution; (2) the membrane; and (3) the applied field (cross flow).

To avoid altering NP properties, such as surface charge, double layer thickness, particle aggregation–disaggregation and dissolution, the chosen carrier solution should mimic the matrix in which the NPs are suspended (*i.e.* pH, ionic strength, *etc.*).[25,35] A bactericide (such as sodium azide) is a common addition.[48] The two most popular membranes used in AF4 are regenerated cellulose and polyethersulphone (PES) with molecular weight cut-offs ranging from 300–10 000 Da. A choice between these focused on minimizing particle–membrane interaction and maximizing sample recovery, which generally occurs by selecting a membrane with same charge as the particles[49] or relying on the surfactant to create uniformly charged NPs and membrane. In preliminary experiments with fresh membranes, similar results were observed for a variety of size cut offs and both membrane compositions. However, the 10 kDa regenerated cellulose gave the most reproducible results with the longest membrane life at approximately 25 fractionations per membrane, and so was used in all subsequent analyses. The cross flow may be considered the key component of analysis as it determines the resolution and quality of separation. The choice of cross flow should be made so that there is a high percent recovery while still having a good separation between void and analyte peaks as well as between different analyte peaks (sizes of particles). As a general rule, high cross flows are used when separating smaller particle sizes while lower cross flows are applied when fractionating larger sizes.

SP-ICP-MS and AF4-ICP-MS comparison

(A) Detection limit

(i) Detection limit, NP size. Size detection limit, here defined as a particle distinguishable as a pulse at least three times the standard deviation above the background, is highly dependent on the ICP-MS being used and to the element of interest (isotopic ratio of mass being measured). To maximize the applicability of the SP-ICP-MS technique to its fullest extent, the sensitivity of the instrument itself is paramount. Newer, more sensitive instruments that have been used for SP-ICP-MS (Perkin Elmer NexION 300Q, Perkin Elmer NexION 300D, Thermo X-Series 2) had the ability to detect NPs as small as 20 nm Ag, as part of the 40 nm particle distribution tail (Fig. 1), while less sensitive instruments, such as the Perkin Elmer Elan 6100, could detect no Ag NP smaller than 80 nm. However, we are undertaking research to develop statistically based methods to deconvolute smaller sized particles from the instrumental and/or dissolved metal background.

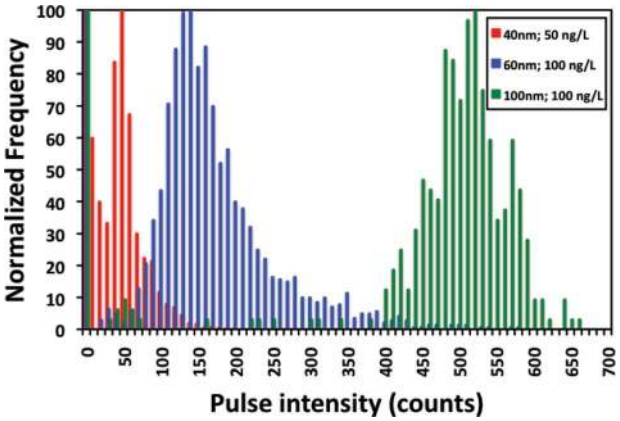

Fig. 1 Pulse intensity *versus* particle number (normalized to the highest frequency) determined by Perkin Elmer NexION 300Q ICP-MS. Each sized NP gives an average pulse intensity with a distribution around the mean, with larger diameter particles registering as higher pulses. For the 40 nm Ag NP distribution, particles of approximately 20 nm are considered the approximate detection limit because lower intensities blend into the instrumental background counts.

The many interchangeable parameters and optimization procedures involved with any FFF method development will allow for variable run conditions. A highlight of the AF4 technique is the capability to separate particles within a 10 to 20-fold size range. The size range (2 nm (ref. 25) to 50 mm (ref. 50)) and separation capability can be altered by varying flow rates and operating conditions.[29,51,52] The purpose of this study was not to determine the smallest possible size detectable by the technique but rather to highlight, in a more general sense, that smaller size fractions could be detected than by the SP-ICP-MS technique.

Differences in the size detection limits of the two techniques warrant further discussion. When using SP-ICP-MS, the pulse registered would be the primary particle size as only the element of interest is being detected. Pulse integration can lead directly to elemental mass, so this negates the possibility of determining if the element is present as an NP bound to larger particles in solution, adhered to humic substances, or is present as an altered particle such as Ag_2S or AgCl. These are important considerations for environmental studies and somewhat limit the interpretations made by SP-ICP-MS analysis. Conversely, since separation in AF4 is related to hydrodynamic diameter, the retention time is based on particle size but may lead to misleading results if the particles become significantly coated or aggregate (such as in high ionic strength solution or in the presence of larger organic particles). Furthermore, interaction with the membrane may delay particle elution from the channel, and in this way may be incorrectly sized. As with any sizing technique, a second form of measurement should be used to ensure correct measurements were made.

(ii) Dynamic range, NP concentrations. Though both SP and AF4-ICP-MS rely on the very sensitive nature of ICP-MS, the applicable concentration ranges for the two techniques are quite different. In particular, SP-ICP-MS requires very low particle

number concentrations to avoid NP coincidence. As the number of particles for a given mass concentration (*i.e.*, ng of nanoparticles per L) increases significantly with decreasing particle size, it is particularly important to ensure that smaller NPs are analyzed *via* SP-ICP-MS at much lower mass-based concentrations.

Using SP-ICP-MS, one could theoretically detect a single particle in as much volume of sample as one is willing to pump through the ICP-MS, though one has to additionally consider the occurrence of false positives. To make any data meaningful, however, a sufficient number of particles should be analyzed to provide a distribution of particle sizes. As a practical matter, it is useful to define a minimum percent of readings that should contain a NP to enable the development of a NP size distribution. Similarly, a maximum percent of readings is useful to ensure, or at least minimize, the likelihood of NP coincidence. As an illustration of this, we determined an approximate concentration detection limit of 2.5 ng L^{-1} for 40 nm Ag NPs (Fig. 2A), or approximately 7.11×10^6 particles per L, which is in line with other studies.[23,43] With a standard data collection time of 120 seconds (t_{total}), a dwell time (d_t) of 0.01 seconds per reading, and instrument settling time of approximately 0.0001 seconds between each reading, the total number of readings (events) collected is 11 770. The number of readings containing pulses corresponding to NPs is the product of the particle number concentration of NPs (N_p; particles per L), the sample flow rate (q_{liq}; L s^{-1}), t_{total}, and the transport efficiency of NPs in the particular ICP-MS system (η_n; unitless). When combined, the fraction of readings, $f(p)$, that should contain NPs can be calculated as:

$$f(p) = \frac{\text{readings containing NPs}}{\text{total readings}} = \frac{N_p q_{liq} t_{total} \eta_\eta}{t_{total}/d_t}$$

Using the typical values of t_{total} and d_t listed above, a 5% transport efficiency, a typical flow rate of 1 mL min^{-1}, the fraction of readings that should be particles is approximately 5.92%. Using this, we can then theoretically determine the concentration based detection limit for other particles sizes. For example, under these same conditions, the detection limit of 100 nm particles would be approximately 40 ng L^{-1}. This is, of course, for simple, monodisperse systems. To avoid coincidence in polydisperse samples and not degrade the quality of distribution obtained from SP-ICP-MS analysis, one could analyze the sample for a longer period of time so as to capture enough NP pulse events to populate a statistically significant distribution. Additionally, increasing the particle transport efficiency will increase the sensitivity of the SP-ICP-MS technique.

As SP-ICP-MS is primarily a particle counting technique, there are instances where a sample contains too many particles. Under these circumstances, multiple smaller particles enter the plasma during one dwell time resulting in fewer, larger pulses, equating to particles of larger size. The upper dynamic range will be dictated by the likelihood of coincident NPs entering the plasma and being detected as a single particle. This is illustrated in Fig. 2B, the 40 nm particles at 100 ng L^{-1} are too concentrated (resulting in a large

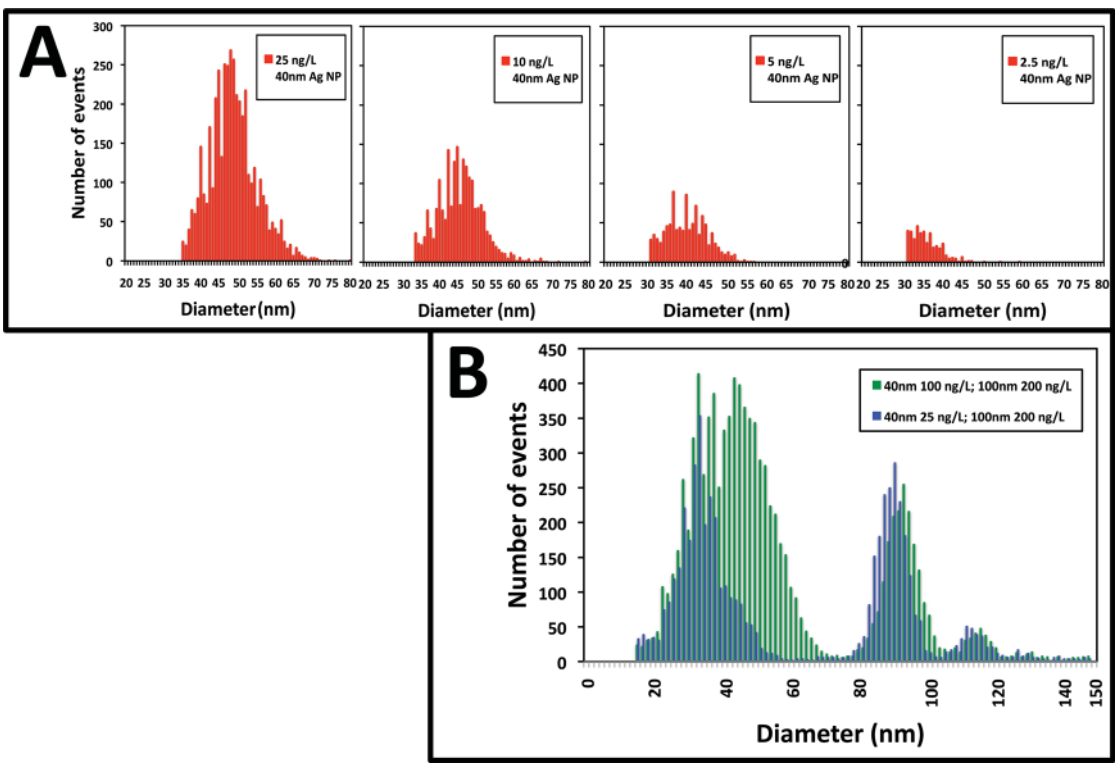

Fig. 2 (A) Dilution scheme of 40 nm Ag NP, using SP-ICP-MS, with approximate detection limit of 2.5 ng L^{-1}. (B) 40 and 100 nm Ag NP mix.40 nm particles at 100 ng L^{-1} are outside SP-ICP-MS dynamic range, observed coincidence of particles. The 40 nm at 25 ng L^{-1} and 100 nm particles are within the acceptable range for the SP-ICP-MS technique.

coincidence of particles), while they are sized correctly when analyzed at 25 ng L^{-1}. While we are not suggesting a hard upper bounds to the percent of readings at this time, it should be noted that the amount of coincidence instances will increase as the fraction of readings that contain particles rise. The extent to which this is acceptable can depend on the type of sample being analyzed, and to the degree of precision one prefers to know the particle distribution. Nonetheless, as long as the fraction of readings containing NPs is approximately 5% of the total readings, one should be able to collect sufficient data to develop an appropriate size distribution as well as minimize the probability of NP coincidence. As an illustration of the importance of NP size in determining this maximum fraction of readings, Fig. 2 also shows correctly sized 100 nm particles run at 200 ppt, which is within the correct dynamic range. Note that these "100 nm particles" were analyzed using differential centrifugation and found to be 90 nm, with a secondary associated particle of 110 nm, and so are sized correctly through this technique.

The dynamic range, as calculated above, should guide one in analyzing unknown samples. For unknown samples where NP size and concentrations are initially unknown, determining the appropriate dynamic range for SP-ICP-MS is somewhat problematic. However, one could determine if the particle number concentration is too high through serial dilution of the sample. With dilution, if the shape of the particle histogram changes with concentration (as illustrated in Fig. 2B, 40 nm particles), then coincidence is likely occurring at the higher concentrations. Conversely, if the sample was truly polydisperse, the histogram should retain its general shape, though the number of events would decrease proportionally with dilution.

With AF4-ICP-MS, analyzed with an injection volume of 100 μL, the detection limit is a much higher mass concentration, at approximately 5 μg L^{-1} (Fig. 3). This is mainly because of the dilution that takes place within the AF4 channel during separation. It is noted, however, that in the given example, a shorter than optimal relaxation time was used, which explains a large amount of NPs eluting in the void (first) peak of the fractogram. By decreasing the elution time, at the sacrifice of resolution, the degree of dilution could be reduced. Other methods of FFF operation, such as post-channel concentration (split flow) or large volume sample introduction (on-channel concentration) may provide a more sensitive analysis, with some studies showing successful characterization with concentration factors as high as 10^5 achieved.[53] Although AF4 is subject to overloading effects like any other analytical separation method, it is highly unlikely that this upper limit for particle concentration would be reached when dealing with NPs in environmental systems.

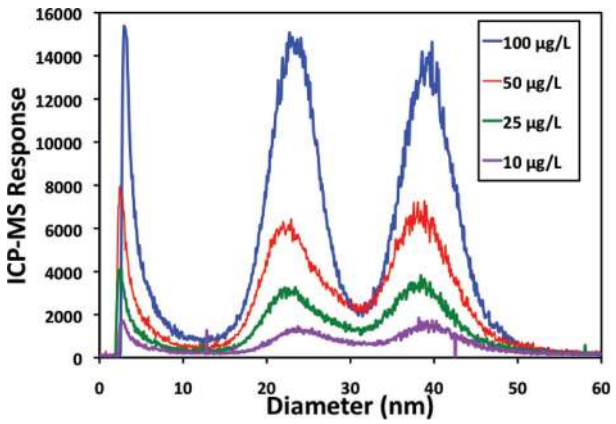

Fig. 3 20 and 40 nm Ag NP mix dilution scheme with AF4-ICP-MS, detection limit approximately 5 μg L^{-1}. ICP-MS: Perkin Elmer 6100. Cross flow 0.7 mL min^{-1}, detector flow 1 mL min^{-1}.

(B) Resolution. The resolution of the SP-ICP-MS technique is fixed by the sensitivity of the ICP-MS instrument, although tuning plays a role as previously described in the discussion of detection limit. Since the pulse intensity generated from the detection of the NP is directly correlated with the NP mass, the differentiation between two differently sized NP is dependent on the ICP-MS detector sensitivity. Furthermore, the resolution between particles is not linear with NP diameter, but rather, with NP mass. The total mass of smaller diameter NPs are more similar than larger diameter NPs. In this way the resolution, in theory, will be better for a larger set of particles, *i.e.* 60 and 80 nm particles would confer better resolution than 40 and 60 nm particles in a given solution. However, this is assuming that the particle distribution for each size is similar, which may not be the case. In Fig. 4, we show good resolution ($R = 0.702$) between the 40 and 80 nm particle mixture (panel A), yet the 60 and 80 nm particles mixture (panel B) was not as well-resolved ($R = 0.492$) due to the breadth of the 80 nm particle distribution. These mixtures of equal particle number (7.11×10^7 particles per L), correspond to 25 ng L^{-1}, 85 ng L^{-1}, and 200 ng L^{-1} for 40, 60, and 80 nm NPs, respectively. When analyzing a mixture of these three particle sizes, and decreasing the concentration of each NP constituent to 3.55×10^7 particles per L to keep the total particle number within the dynamic range of the SP-ICP-MS technique, similar resolution is achieved between the 60 and 80 nm ($R = 0.499$) as the two-particle mixtures (Fig. 4, panel C), with good resolution between the 40 and 60 nm particles ($R = 1.05$).

For AF4-ICP-MS analysis there is a linear relationship between NP diameter and retention time so there is no differential resolution improvement due to size as with SP-ICP-MS. However, as discussed previously, there are a multitude of choices that will directly affect the separation quality in the AF4 channel (Fig. 5). For example, when analyzing 20 and 40 nm particles of equal concentration, although peak breadths at 1 mL min^{-1} cross flow, 1 mL min^{-1} detector flow are narrower, the run conditions 1.25 mL min^{-1} cross flow, 0.5 mL min^{-1} detector flow provide superior resolution. For the present study, conditions were chosen to be able to achieve nearly baseline resolution for 20 and 40 nm Ag NP for comparison to SP-ICP-MS, with 1 mL min^{-1} detector flow and 0.7 mL min^{-1} cross flow. This mixture was also used as a daily standard to test membrane quality and flow conditions, resulting in our "standard run conditions" resolution of 1.13. This resolution is slightly reduced when analyzing a mixture of 40, 60, and 80 nm (40 : 60 mix $R = 0.876$; 60 : 80 mix $R = 0.744$) particles of equal concentration (20 μg L^{-1}, each constituent) shown in Fig. 6, where the cross flow was increased to 1 mL min^{-1} to account for particle sizes being more similar. In contrast to SP-ICP-MS, each analyte peak can be quantified individually through the increased resolution. However, it is noted that the increased breadth of the 80 nm

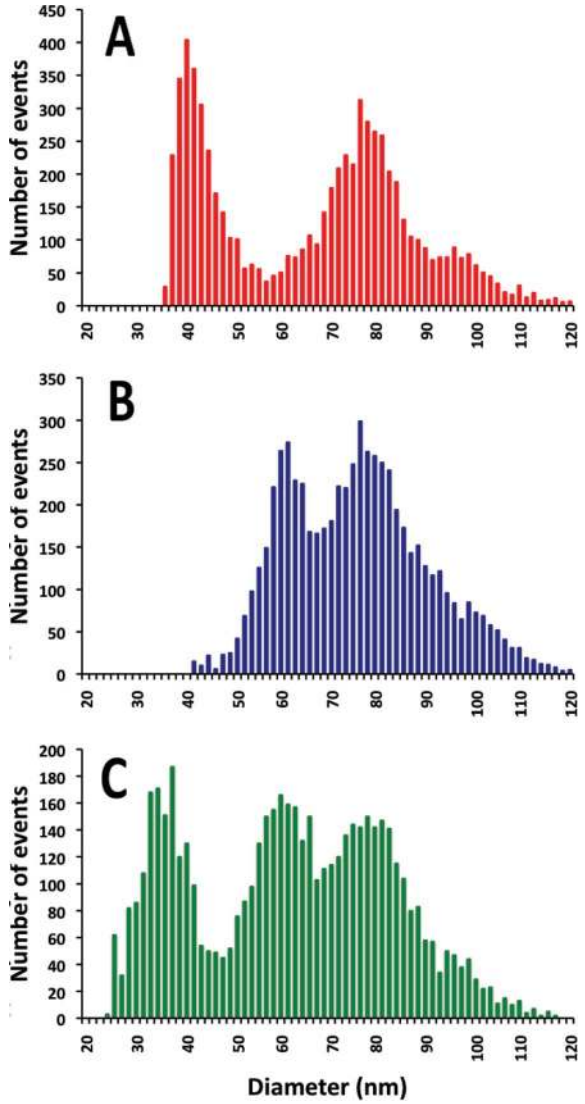

Fig. 4 Detection of Ag NP mixtures using SP-ICP-MS. Equal particle number (7.11×10^7 particles per L, panels A and B) for each constituent. Mixtures of 40 and 80 nm particles (A), and 60 and 80 nm particles (B), conferring a resolution of 0.702 and 0.492 respectively. (C) Equal particle number mixture (3.55×10^7 particles per L) of 40, 60, and 80 nm particles with similar resolution to the two particle samples.

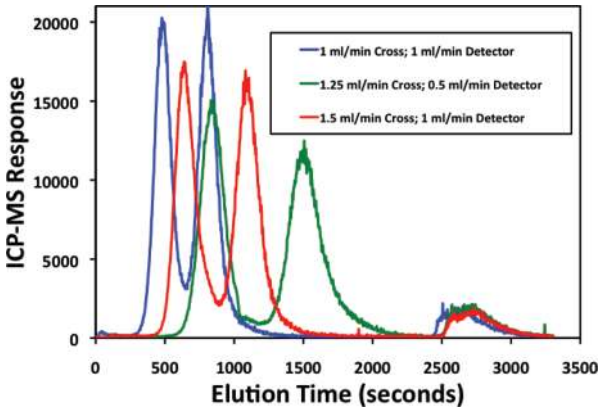

Fig. 5 Change of flow conditions changes resolution between particle sizes, here 20 and 40 nm Ag NPs. Run conditions can be chosen so that peak breadth is smaller, or better resolution achieved, depending on experimental needs. ICP-MS: Perkin Elmer 6100.

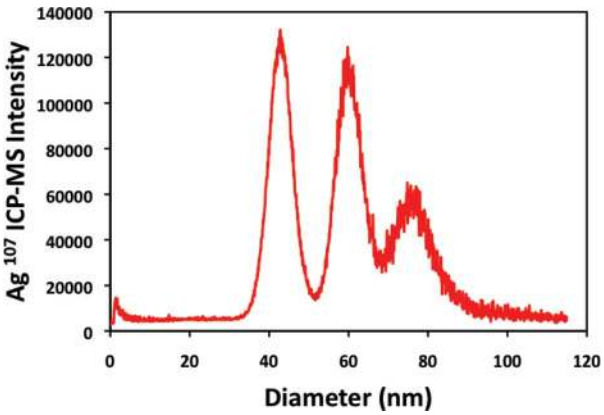

Fig. 6 Mixture of 40, 60, and 80 nm Ag NPs (20 μg L^{-1}, each constituent), with flow conditions of 1 mL min^{-1} detector flow and 1 mL min^{-1} cross flow. ICP-MS: Perkin Elmer NexIONQ.

peak, in relation to the other particle sizes, is maintained from the SP results. Furthermore the decrease in recovery with particle size is not unusual in AF4 analysis.

(C) Multi-form analysis

(i) Dissolved versus *NP constituents.* For differentiating dissolved from nanoparticulate elements there is a clear advantage in using SP-ICP-MS over AF4-ICP-MS, as any dissolved constituent moves through the membrane and cannot be quantified in the latter technique. However, distinguishing between dissolved background and NP pulses in SP-ICP-MS is not a trivial task. We have suggested in previous work,[21] using an iterative algorithm to qualify a NP pulse as at least three sigma above the dissolved background. Although this method may still be theoretically valid in some instances, we found that with more sensitive instruments pulses correlating to NPs register at higher intensities and therefore skew the distribution of readings so that the three sigma qualification to register a pulse as a NP is set too high, and NPs are therefore incorrectly classified as background. In these circumstances, the iterative method is abandoned and the raw data are plotted as pulse intensity as a function of pulse number, where any values below the first minimum in the histogram were considered background/dissolved constituent, and values higher than the first minimum were considered NP pulses. It is noted, however, that the term dissolved metal is used operationally in this context to refer to both Ag^+ and any Ag NP that is smaller than can be distinguished as a NP by the SP-ICP-MS method at this time.

The concentrations of Ag^+ and NP can be independently quantified in a given sample. An increasing concentration of Ag^+ can be recognized by an increase in intensity of the lower intensity counts. Once the dissolved Ag is distinguished from the Ag NP pulses, the background intensity can be directly compared to the calibration curve to quantify the concentration of dissolved metal in the sample. In solutions containing both dissolved and Ag NPs, the Ag-NP pulse would register as the summation of Ag^+ background and Ag–NP pulse intensities, *i.e.*

the intensities are additive. Since the increase of dissolved metal not only presents itself by increasing the background concentration at low counts, but also by shifting the NP pulses to higher intensities, Ag–NP can be correctly sized only after subtracting the background intensity from the Ag–NP pulse intensity before sizing. In Fig. 7, we show the addition of increasing Ag^+ (0, 50, and 100 ng L^{-1}) to 100 nm Ag NP (100 ng L^{-1}). As the dissolved constituent increases, we note the background moves to proportionally higher intensities. In addition, the NP histogram shifts to higher intensities as well. As shown in Table 1, regardless of any increase in Ag^+ background, the adjusted pulse intensity is the same in each analysis, and so the NP can be independently sized regardless of Ag^+ concentration in the sample. Again, keeping in mind that nominal "100 nm particles" were determined to in fact be 90 nm, SP-ICP-MS is apt to adequately size these Ag^+/Ag NP mixtures.

(ii) NP complexes. The AF4 technique has an advantage over SP-ICP-MS when studying small sized complexes or, possibly, for the study of NP aggregation. In a 20, 40 nm Ag NP mixture (100 μg L^{-1}) dispersed in DI water, we were able to detect surface modifications to Ag NPs with the addition of BSA to solution (Fig. 8). We noticed an initial increase of particle diameter (approximately 5 nm) from the daily standard (20, 40 nm Ag NP mixture in DI water, yellow trace) in the first analysis of Ag NP coated with BSA (red trace). Analysis over the following hours (green and purple traces) showed the slight dissolution of NP, indicated by the decrease in particle diameter. The freed Ag^+ released from the NP was subsequently complexed to the excess BSA in solution, as evidenced by the increasing formation of small sized particles (first peak) over time. In this way, we were able to quantify protein bound free silver ions in solution.

(iii) Multiple metals analysis. By design, SP-ICP-MS is best suited to analyze one metal at a time in an individual NP. Therefore, multiple metal analysis is not preferable, at least not in one run. However, the capability of multi-metal analysis by spectroscopy is an added benefit when combined with the continuous fractionation of AF4. The resultant hyphenation of AF4-ICP-MS provides nanoparticle sizing, detection, and compositional analysis capabilities at the parts per billion level, which is critical to environmental and toxicological investigations of nanomaterials. Furthermore, an increased knowledge about size-dependent variations in composition and trace element interactions may interest those working in areas

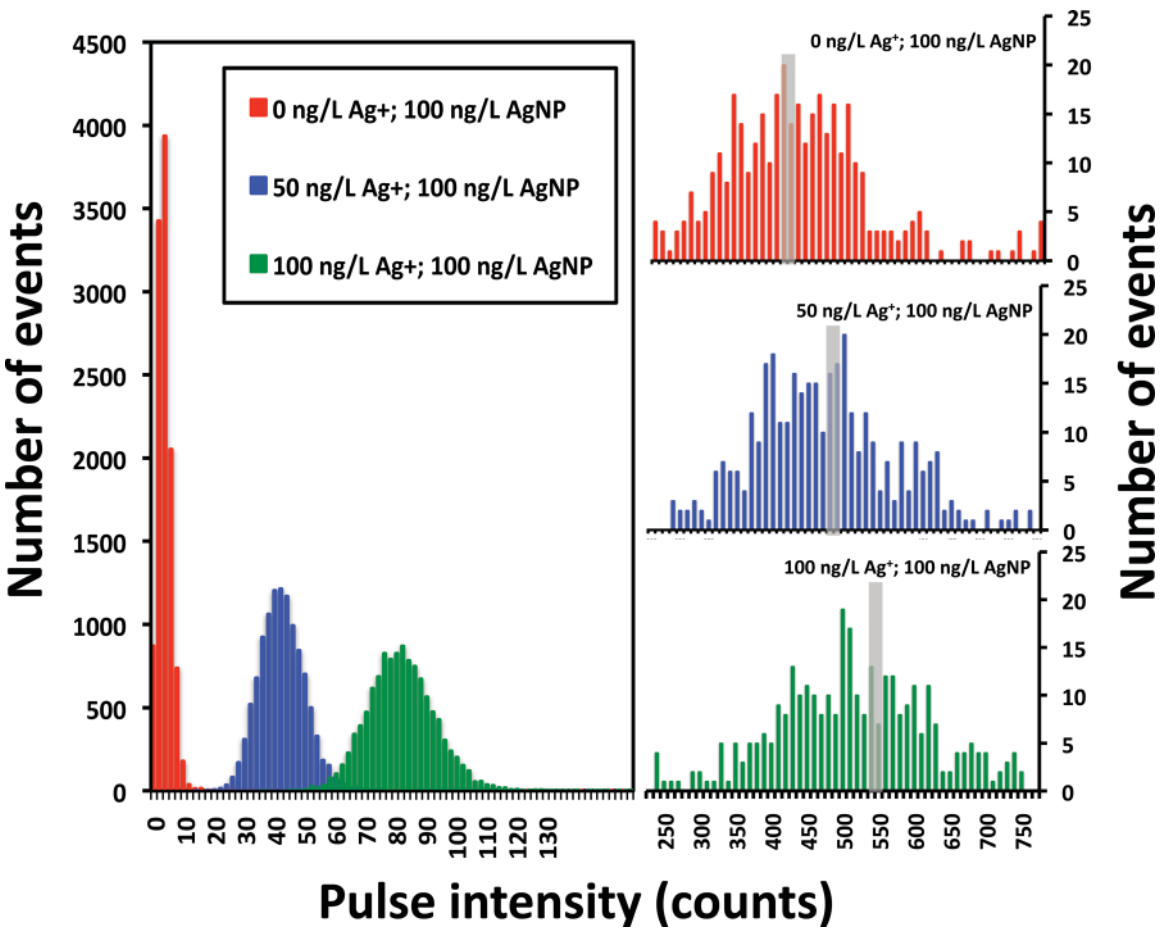

Fig. 7 Binned pulse intensity *versus* frequency for addition of dissolved Ag^+ and 100 nm Ag NP mixtures. Left panel depicts increasing background concentration, right three panels show increasing pulse intensity for the 100 nm Ag NPs with increasing background intensity, where grey bar indicates median particle number.

Table 1 Adjustment of background correction to NP pulse intensity to correctly size Ag NP with increased concentrations of dissolved Ag

Sample	Average background (count)	Concentration (ng L^{-1})	Avg NP pulse intensity	Background corrected pulse intensity	Calculated diameter (nm)
0 ng L^{-1} Ag^+; 100 ng L^{-1} 100 nm NP	6 ± 2.3	6.3	459	453	83 ± 12.9
50 ng L^{-1} Ag^+; 100 ng L^{-1} 100 nm NP	44 ± 7.5	53.2	502	458	82 ± 13.2
100 ng L^{-1} Ag^+; 100 ng L^{-1} 100 nm NP	78 ± 10.8	94.5	561	483	84 ± 16.1

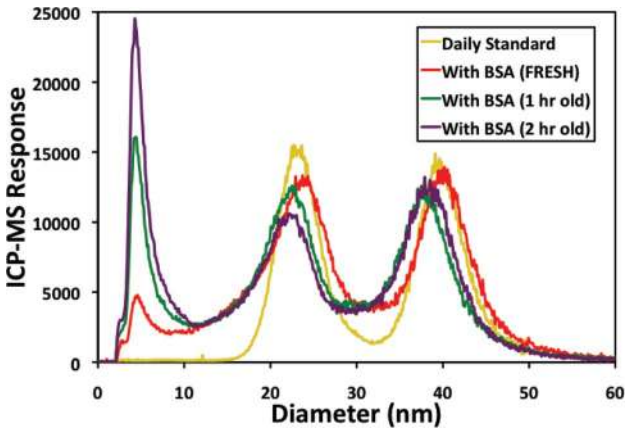

Fig. 8 AF4-ICP-MS fractogram depicting daily 20 and 40 nm Ag NP standards in DI water (yellow trace). Coating of Ag NP with BSA (blue trace) and subsequent dissolution of Ag NP and tracking of accumulation of protein bound Ag^+ (red, green, and purple traces).

concerning methods for characterization of NP interactions in risk evaluation. This advantage is highlighted particularly well by Pace *et al.*,[37] in a nanoecotoxicity study.

Advantages and limitations of using SP-ICP-MS in NP characterization

As primarily a counting and sizing technique, the main advantage of SP-ICP-MS over other techniques is its high sensitivity. Size and particle number data can easily and accurately be obtained at sub-μg L^{-1} concentration levels for a variety of metallic NPs. Furthermore, the technique can differentiate the particle of interest from other incidental particles of the same size, but different composition, by its element specificity. This is true even in complex systems. Distinguishing dissolved from nanoparticulate constituents of a given metal is another distinct advantage of SP-ICP-MS. Additionally, SP-ICP-MS can provide better resolution than many of the currently available instruments for sizing, especially when considering the environmentally relevant concentrations at which the method operates. From a practical standpoint, the data collection parameters are similar to traditional ICP-MS operational procedures and so require little additional training. Furthermore, as SP-ICP-MS utilizes a relatively standard laboratory instrument and no additional equipment, laboratories would not incur extra costs in performing this type of analysis. On the other hand, presently, the smallest detectable particle may be larger than many particles of interest and so may exclude this technique as a viable option under some experimental conditions. However, efforts are currently underway to deconvolute smaller sized NP from background intensities. Certainly, SP-ICP-MS is a promising technique for nanoparticle metrology that has the ability to address many of the current analytical challenges that are faced in characterizing nanomaterials in a number of complex matrices including environmental, biological, and food samples.

Advantages and limitations of using AF4-ICP-MS in NP characterization

Since its conception, the development of field flow fractionation has progressed to have numerous applications that demonstrated the versatility of the technique, yet until recently had not found widespread use for quantitative environmental applications. Today, researchers in the fields of nanoscience, nanotechnology, and biotechnology are eager to try new metrologies and analytical methods that can size particles in the range and with the precision that FFF can perform. AF4 can detect very small particles over a wide size range, with superb resolution, and when coupled to ICP-MS has element specific capabilities, including mixed metals analysis. The ability to detect small size changes allows one to validate coating thickness on the surface of NPs as well as determine the extent of complexation and aggregation of NP in a variety of matrices. However, the lengthy method development process and extra cost may be a drawback to some laboratories. The detection limit, although improved with the hyphenation to ICP-MS than with previous couplings such as UV-VIS, DLS, or fluorescence detectors, is high due to the dilution that takes place within the channel. Some concentration techniques may be applied either before analysis or by loading the channel, yet this is beyond the scope of the present study. Nevertheless, FFF (and consequently AF4-ICP-MS) has become more of a mainstream analytical technique for separating and characterizing analyte species for physiochemical changes for many particles, including NP. This will, in time, provide the method development and method refinement necessary for making the implementation of FFF a less time consuming task.

Conclusions

There is a need to determine NP behavior, aggregation, complexation, and dissolution because different fate and transport predictions for environmental and biological effects depend on the NP state when exposure occurs. It is unlikely that NPs will remain as they were when manufactured during their entire lifecycle (creation, use, transport, final fate).[54] The transformations that occur, as well as when and under what conditions they occur, should be evaluated so as to enable the appropriate human and ecological risk analysis. Here, SP-ICP-MS and AF4-ICP-MS were able to describe a number of NP properties that are specifically relevant to environmental and

toxicological studies, such as size, concentration, associated dissolved constituents, coatings, and complexation. However, each technique has specific strengths, which prove valuable for defining a given set of NP characteristics, as well as limitations that are inherent to each technique.

Future development in the areas of SP-ICP-MS and AF4-ICP-MS

For those in the nanotechnology community, there are many current knowledge gaps in regards to the release, environmental transformation, and potential toxicity of engineered NPs. New analytical techniques are under development that will enable more rapid, sensitive, and specific detection for an array of these products, both in the lab and in more complex field and biological samples. Many of the method details of SP-ICP-MS have been developed so that, at least, researchers can now use the technique to be implemented beyond the laboratory and should now focus on application to real world samples. To strengthen SP now, a more sensitive ICP-MS, such as the single element sector field HR-ICP-MS, may enable detection of smaller sized NPs.[11] Development of time-of-flight (TOF-ICP-MS) could overcome the current SP-ICP-MS limitation of only single element detection. There has been suggestion of coupling SP-ICP-MS with chromatography-like techniques, such as FFF, as well as hydrodynamic chromatography, to pre-sort constituents of complex samples. Although there is a large dilution factor with FFF separation, this is not a concern for SP-ICP-MS as dilute samples are a prerequisite for analysis. Indeed, as a stand-alone technique or coupled to FFF, SP-ICP-MS shows particular promise in the field of nanometrology, both for manufactures of nanoparticles and nanoproducts to conduct quality assurance tests, and as the demand to characterize more complex and varied samples arise in the quest to determine the environmental and biological impacts of nanotechnology.

Acknowledgements

We would like to thank the funding sources, by which this research was made possible. Army Corps of Engineers, grant number W912HZ-09-P-0163 and the National Institute of Health Sciences, grant number DE-FG02-08ER64613.

Notes and references

1 N. Mueller and B. Nowack, *Environ. Sci. Technol.*, 2008, **42**, 4447–4453.
2 F. Gottschalk, T. Sonderer, R. Scholz and B. Nowack, *Environ. Sci. Technol.*, 2009, **43**, 9216–9222.
3 B. Nowack, *Nano Today*, 2009, **4**, 11–12.
4 S. Blaser, M. Scheringer, M. MacLeod and K. Hungerbühler, *Sci. Total Environ.*, 2008, **390**, 396–409.
5 J. Morones, J. Elechiguerra, A. Camacho, K. Holt, J. Kouri, J. Ramirez and M. Yacaman, *Nanotechnology*, 2005, **16**, 2346.
6 M. Auffan, J. Rose, J. Bottero, G. Lowry, J. Jolivet and M. Wiesner, *Nat. Nanotechnol.*, 2009, **4**, 634–641.
7 P. Christian, F. Von der Kammer, M. Baalousha and T. Hofmann, *Ecotoxicology*, 2008, **17**, 326–343.
8 S. Pal, Y. Tak and J. Song, *Appl. Environ. Microbiol.*, 2007, **73**, 1712.
9 S. Luoma, *Woodrow Wilson International Center for Scholars, Project on Emerging Nanotechnologies*, The PEW Charitable Trusts, Washington, DC, 2008.
10 A. M. E. Badawy, T. P. Luxton, R. G. Silva, K. G. Scheckel, M. T. Suidan and T. M. Tolaymat, *Environ. Sci. Technol.*, 2010, **44**, 1260–1266.
11 F. von der Kammer, P. L. Ferguson, P. A. Holden, A. Masion, K. R. Rogers, S. J. Klaine, A. A. Koelmans, N. Horne and J. M. Unrine, *Environ. Toxicol. Chem.*, 2012, **31**, 32–49.
12 G. Leppard, D. Mavrocordatos and D. Perret, *Water Sci. Technol.*, 2004, **50**, 1.
13 Y. Song, V. Jimenez, C. McKinney, R. Donkers and R. W. Murray, *Anal. Chem.*, 2003, **75**, 5088–5096.
14 D. Y. Lyon, L. K. Adams, J. C. Falkner and P. J. J. Alvarez, *Environ. Sci. Technol.*, 2006, **40**, 4360–4366.
15 K. W. Powers, M. Palazuelos, B. M. Moudgil and S. M. Roberts, *Nanotoxicology*, 2007, **1**, 42–51.
16 K. A. Howell, E. P. Achterberg, A. D. Tappin and P. J. Worsfold, *Environ. Chem.*, 2006, **3**, 199–207.
17 A. Akthakul, A. I. Hochbaum, F. Stellacci and A. M. Mayes, *Adv. Mater.*, 2005, **17**, 532–535.
18 K. Tiede, A. Boxall, S. Tear, J. Lewis, H. David and M. Hassellov, *Food Addit. Contam.*, 2008, **25**, 795–821.
19 J. R. Lead and K. J. Wilkinson, *Environ. Chem.*, 2006, **3**, 159–171.
20 M. Hasselloev, J. Readman, J. Ranville and K. Tiede, *Ecotoxicology*, 2008, **17**, 344–361.
21 D. M. Mitrano, E. K. Lesher, A. J. Bednar, J. Monserud, C. P. Higgins and J. F. Ranville, *Environ. Toxicol. Chem.*, 2012, **31**, 115–121.
22 H. E. Pace, N. J. Rogers, C. Jarolimeck, V. A. Coleman, C. P. Higgins and J. F. Ranville, *Anal. Chem.*, 2011, **83**, 9361–9369.
23 F. Laborda, J. Jiménez-Lamana, E. Bolea and J. R. Castillo, *J. Anal. At. Spectrom.*, 2011, **26**, 1362–1371.
24 J. Ranville, D. Chittleborough, F. Shanks, R. Morrison, T. Harris, F. Doss and R. Beckett, *Anal. Chim. Acta*, 1999, **381**, 315–329.
25 M. Baalousha and J. Lead, *Environ. Sci. Technol.*, 2007, **41**, 1111–1117.
26 R. Beckett and B. T. Hart, *Environ. Part.*, 1993, **2**, 165–205.
27 M. H. Moon, D. Kang, J. Jung and J. Kim, *J. Sep. Sci.*, 2004, **27**, 710–717.
28 E. Bolea, J. Jimenez-Lamana, F. Laborda and J. Castillo, *Anal. Bioanal. Chem.*, 2011, 1–10.
29 J. C. Giddings, *Science*, 1993, **260**, 1456.
30 C. W. Isaacson and D. Bouchard, *J. Chromatogr., A*, 2010, **1217**, 1506–1512.
31 M. Hassellöv, F. der Kammer and R. Beckett, *Environmental Colloids and Particles*, 2007, pp. 223–276.
32 P. Reschiglian, A. Zattoni, B. Roda, E. Michelini and A. Roda, *Trends Biotechnol.*, 2005, **23**, 475–483.
33 B. Roda, A. Zattoni, P. Reschiglian, M. H. Moon, M. Mirasoli, E. Michelini and A. Roda, *Anal. Chim. Acta*, 2009, **635**, 132–143.
34 S. K. R. Williams, J. R. Runyon and A. A. Ashames, *Anal. Chem.*, 2011, **83**, 634–642.
35 M. Baalousha, B. Stolpe and J. Lead, *J. Chromatogr., A*, 2011, **1218**, 4078–4103.
36 M. Bouby, H. Geckeis and F. Geyer, *Anal. Bioanal. Chem.*, 2008, **392**, 1447–1457.
37 H. E. Pace, E. K. Lesher and J. F. Ranville, *Environ. Toxicol. Chem.*, 2010, **29**, 1338–1344.
38 A. Poda, A. Bednar, A. Kennedy, A. Harmon, M. Hull, D. Mitrano, J. Ranville and J. Steevens, *J. Chromatogr., A*, 2011, **1218**, 4219–4225.
39 B. Schmidt, K. Loeschner, N. Hadrup, A. Mortensen, J. J. Sloth, C. Bender Koch and E. H. Larsen, *Anal. Chem.*, 2011, **83**, 2461–2468.
40 S. Tadjiki, S. Assemi, C. E. Deering, J. M. Veranth and J. D. Miller, *J. Nanopart. Res.*, 2009, **11**, 981–988.
41 M. Delay, T. Dolt, A. Woellhaf, R. Sembritzki and F. H. Frimmel, *J. Chromatogr., A*, 2011, **1218**, 4206–4212.
42 K. Songsilawat, J. Shiowatana and A. Siripinyanond, *J. Chromatogr., A*, 2010, **1218**, 4213–4218.
43 H. E. Pace, N. J. Rogers, C. Jarolimeck, V. A. Coleman, C. P. Higgins and J. F. Ranville, *Anal. Chem.*, 2011, **83**, 9361–9369.
44 C. Degueldre and P. Favarger, *Colloids Surf., A*, 2003, **217**, 137–142.
45 C. Degueldre and P. Favarger, *Talanta*, 2004, **62**, 1051–1054.
46 C. Degueldre, P. Favarger and S. Wold, *Anal. Chim. Acta*, 2006, **555**, 263–268.
47 C. R. Thomas, S. George, A. M. Horst, Z. Ji, R. J. Miller, J. R. Peralta-Videa, T. Xia, S. Pokhrel, L. Ma dler and J. L. Gardea-Torresdey, *ACS Nano*, 2011, **5**, 13–20.

48 M. Baalousha, F. Kammer, M. Motelica-Heino and P. Le Coustumer, *J. Chromatogr., A*, 2005, **1093**, 156–166.
49 E. Bolea, M. Gorriz, M. Bouby, F. Laborda, J. Castillo and H. Geckeis, *J. Chromatogr., A*, 2006, **1129**, 236–246.
50 S. K. Ratanathanawongs and J. C. Giddings, *PROCESS-RENNES-*, 1993, **521**, 13.
51 J. Giddings, F. Yang and M. N. Myers, *Science*, 1976, **193**, 1244.
52 M. E. Schimpf, K. Caldwell and J. C. Giddings, *Field-Flow Fractionation Handbook*, Wiley-Interscience, New York, 2000.
53 H. Lee, S. K. R. Williams and J. C. Giddings, *Anal. Chem.*, 1998, **70**, 2495–2503.
54 B. Nowack, J. F. Ranville, S. Diamond, J. A. Gallego-Urrea, C. Metcalfe, J. Rose, N. Horne, A. A. Koelmans and S. J. Klaine, *Environ. Toxicol. Chem.*, 2012, **31**, 50–59.

